

Experimental Study of Spatial and Temporal Dynamics in Double Phase Conjugation

Tong Kun Lim*, Keumcheol Kwak†, and Daeun Lee

Department of Physics, Korea University, Seoul 136-701, KOREA

Young Hun Yu‡

Department of Physics, Cheju University, Cheju 690-756, KOREA

Jung Young Son

3D Imaging Media Group, Korea Institute of Science and Technology, Seoul 136-791, KOREA

(Received February 19, 1999)

Spatial and temporal dynamics arising in a photorefractive crystal (BaTiO_3) during the process of double phase conjugation was studied experimentally. We studied the dynamical effects caused by the buildup of the diffraction grating and turn on of phase conjugated beams, as well as the spatial effects caused by the finite transverse coupling of beams and the propagation direction of beams. We observed conical emission in DPCM. We believe that various temporal and spatial instabilities are due to movement of the nonlinear grating. For a real beam coupling and constructive interaction of interference fringes in the crystal, we observed steady, periodic, irregular temporal behavior. And, by the calculation of the correlation index, we found that the spatial correlation decreased as the transverse interaction region was increased.

I. INTRODUCTION

Optical phase conjugation in photorefractive crystals still attracts great attention because of its numerous potential applications in optical signal processing, wave front correction, optical communication and optical neural networks application. There has recently been great interest in determining the conditions under which nonlinear optical systems may become unstable since the instability can be a limiting factor of the performance and applications of such devices. Intensive studies of the properties of Phase Conjugation Mirrors (PCM) have shown that temporal irregular fluctuations in the phase conjugated output intensity depends on the input intensity and especially on the internal interaction geometry. Also, a nonlinear system with a region of instabilities and possible transition to chaos presents an interesting subject in the field of nonlinear optics. There are various geometric configurations for PCM [1–3]. Among them, the Double Phase Conjugation Mirror (DPCM) [4–8] is a popular wave mixing

geometry for phase conjugation of mutually incoherent light beams in photorefractive media. In this geometry two mutually incoherent light beams which are incident upon opposite faces of a photorefractive crystal, can produce two phase conjugated beams. The DPCM was first suggested and demonstrated by Cronin-Golomb *et al.* [4]. In this process, as the interaction region of the two input beams increases, the PC beam becomes unstable temporally and spatially. D. J. Gauthier [9] suggested a model to explain the temporal and spatial instability when the beams interact in a single crystal. But the instability of PC in a single crystal is not clearly understood yet. And in our experiment, we observed conical emission in DPCM occasionally. The conical emission has the extraordinary polarization and there are many spatial patterns in the conical emission. The spatial pattern in conical emission becomes complex (spatial chaos) as the interaction region of the two entrance beams is increased. Some people do not regard the conical emission as a pure phase conjugation beam [10]. But through our experiment, we think that this state is in the transient process of spatio-temporal chaos since the expanded beam shows the composite of many complex patterns and the dynamics of it has the route to chaos. So in this paper we investigated the

*e-mail: tklim@qopt.korea.ac.kr

†e-mail: kkwak@qopt.korea.ac.kr

‡e-mail: yhyoung@cheju.cheju.ac.kr

temporal instability and spatial instability in a Double Phase Conjugation Process as a function of interaction region. We have varied the launching beam location, and incident angle to change the interaction region and varied Fresnel number to change the transverse interaction region. Also we studied the route to spatial instability by spatial coherence index.

II. THEORY

Figure 1 shows a DPCM. Pump beams, A_2 and A_4 enter the crystal in opposite directions and the phase conjugated beams are generated. A_1 is the PC of the A_2 and A_3 is the PC of the A_4 . To represent the DPCM process we introduce a four wave mixing(4WM) process in the paraxial approximation and the crystal thickness d and the beam spot size. And we can write the dimensionless equation(Eq. 1) [10].

$$\begin{aligned} \partial_z A_1 + \beta \hat{K} \cdot \nabla_T A_1 + i\phi \nabla_T^2 A_1 &= Q A_4, \\ \partial_z A_2 + \beta \hat{K} \cdot \nabla_T A_2 - i\phi \nabla_T^2 A_2 &= \bar{Q} A_3, \\ \partial_z A_3 - \beta \hat{K} \cdot \nabla_T A_3 - i\phi \nabla_T^2 A_3 &= -Q A_2, \\ \partial_z A_4 - \beta \hat{K} \cdot \nabla_T A_4 + i\phi \nabla_T^2 A_4 &= -\bar{Q} A_1, \end{aligned} \quad (1)$$

where A_j and Q denote the amplitudes of beams and that of the transmission grating, respectively, β is the relative transverse displacement(caused by the noncollinear propagation of the four beams), \hat{K} is the wave vector($\hat{K}_{14} = \mathbf{k}_1 - \mathbf{k}_4$ or $\hat{K}_{32} = \mathbf{k}_3 - \mathbf{k}_2$) and ϕ is the controlling parameter for the diffraction in the crystal. In scaled coordinates $\beta = \theta/\sqrt{2}\delta$, where θ is the small half angle between the incident beams, $\delta = (\omega_0/d)$ is the beam's angular spread and $\phi (= 1/4\pi F)$ is related to the Fresnel number $F = \omega_0^2/\lambda d$. $K \cdot \nabla_T$ is the directional derivative in the transverse(x, y) plane along the grating wave vector \hat{K} .

Normally θ , δ , and ϕ are small, so that the mixed derivative correction to the transverse Laplacian can be neglected. However, the convective term $\partial_x A_j$ cannot be neglected because the quantity $\theta/\delta (= \beta)$ need not be small. From Eq. 1, we can see that the PC beams depend on the amplitude, the ratio of the entrance beams, the beam spot size and the angle of the entrance beam. The PC beam can be generated if the

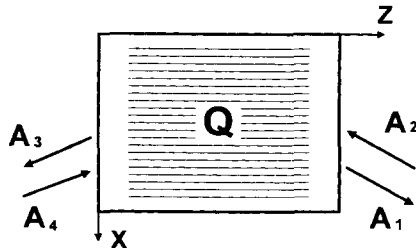


FIG. 1. Double Phase Conjugation Mirror.

condition $\hat{K}_{14} = \hat{K}_{32}$ is satisfied from Eq. 1. If the entrance beam is plane wave, the possible PC beams satisfying the condition $\hat{K}_{14} = \hat{K}_{32}$ can be infinite. That is, the solutions form the cylindrically symmetric vector having the center at the axis in the direction of $\mathbf{k}_4 - \mathbf{k}_2$. Therefore when the gain of conic scattering is similar to that of the conjugated beam for the plane wave, a circular beam is observed in the process of MPPC(mutually pumped phase conjugation). But if the A_j have the spatial distribution, not plane wave, there is the relation between A_j and wave vector \mathbf{k} , i.e.,

$$\nabla^2 A - 2i(\mathbf{k} \cdot \nabla)A = 0. \quad (2)$$

If the entrance beam is not plane wave, the PC beam satisfying Eq. 2 and $\hat{K}_{14} = \hat{K}_{32}$ is unique. Therefore the spatial distribution of the entrance beam is important to the fidelity of the PC beam [12] and the temporal evaluation of Q is approximated by a relaxation equation of the form,

$$\tau \frac{\partial Q}{\partial t} + \frac{E_D + E_q + iE_0}{E_M + E_D + iE_0} Q = \frac{\gamma}{I_0} (A_1 \bar{A}_4 + \bar{A}_2 A_3), \quad (3)$$

$$\gamma = \gamma_0 \frac{E_q + E_D}{E_D} \frac{E_D + iE_0}{E_M + E_D + iE_0}, \quad (4)$$

where τ is the response time of the grating formation, I_0 is the total intensity, γ is the coupling strength[(coupling constant) \times (crystal thickness)], E_D , E_q , E_M are the characteristic electric fields of the photorefractive crystal and E_0 is the external electric field. In the case that E_0 is zero, the phase difference between the interference pattern($A_1 \bar{A}_4 + \bar{A}_2 A_3$) and Q is $\pi/2$. If E_0 is not zero, the coupling constant becomes complex and the phase difference is no longer $\pi/2$ and the interference pattern in the crystal moves. This process generates the spatio-temporal instability of the PC beam.

III. EXPERIMENTAL SETUP

The experimental setup is shown in Fig. 2. The dimension of the BaTiO₃ crystal was 5.0 mm \times 4.6 mm \times 4.15 mm and it had been electrically poled into a single ferroelectric domain. The input beam source was a 5 W Ar⁺ laser operated at 514.5 nm.

The photodiodes were used for the temporal behavior and the spatial correlation of the PC beams. Also a CCD camera was used for the spatial pattern configuration of the PC beam. The entrance beam spot size incident on the crystal was fixed to be 0.8 mm. Fig. 3 shows the configuration of entrance beam and crystal. The laser beam entered from opposite sides and the angle between the entrance beams and c-axis of the crystal are α and β .

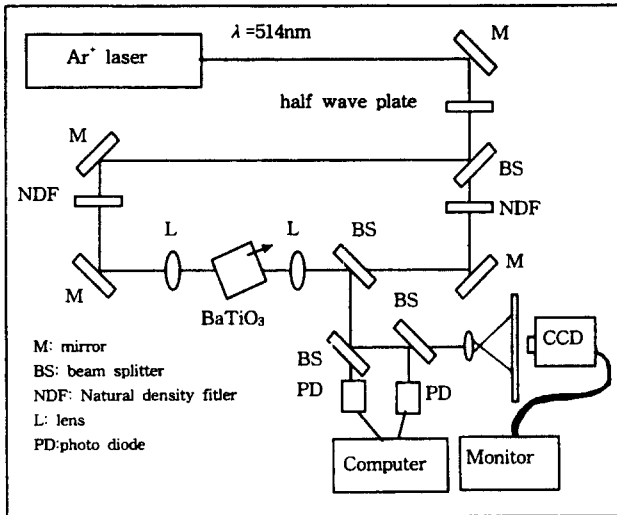


FIG. 2. Scheme of experimental setup.

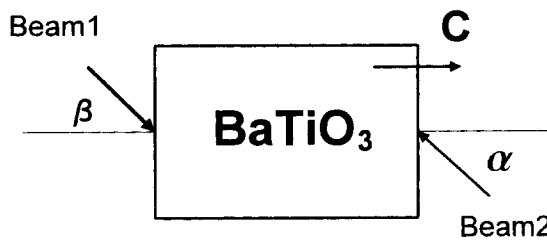


FIG. 3. DPCM geometry of entrance beams and crystal.

IV. EXPERIMENTAL RESULT AND DISCUSSION

First, we measured the temporal behavior of the PC beam as a function of interaction region of two beams. We fixed the one entrance beam angle α to 20° and we changed the angle β of the other beam. In this case we fixed the diameter of the entrance beam. Fig. 4 shows the temporal behavior of the PC beam as β is changed. When β is larger than 47° , the PC output intensity is stable. But when β is smaller than 47° the output beam intensity becomes temporally unstable. The temporal behavior of the PC beam intensity goes from periodic through quasi-periodic and chaotic states as β is decreased. Fig. 5 is the power spectrum of Fig. 4. In Fig. 5, when the entrance angle is 42° , there is single frequency. When the entrance angle is decreased, many frequency components are created and the spectrum is broadened. This result confirmed that the temporal signal becomes more complex as the entrance angle is decreased (that is, the interaction region is increased). Fig. 6 shows the spatial pattern of the PC beam when the entrance angle condition is the same as Fig. 4. Fig. 6(a) shows the pure phase conjugated beam. The spatial pattern becomes complex and spreads out like a bird wing as the entrance angle is de-

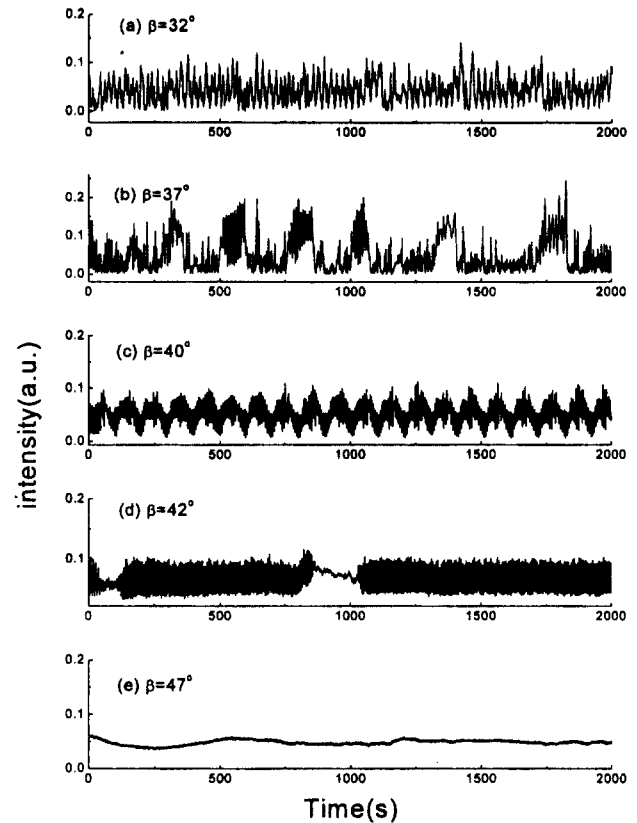
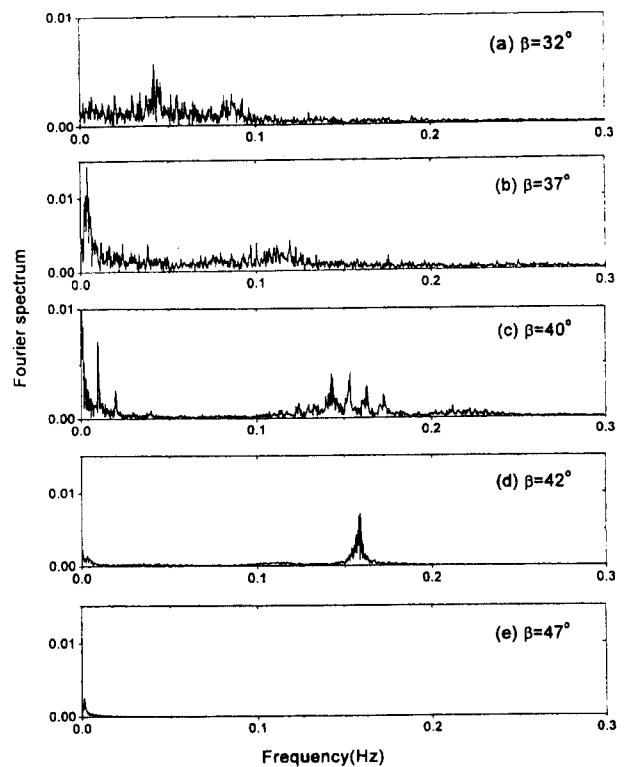

 FIG. 4. Temporal Behavior of PC when one entrance angle is fixed ($\alpha = 20^\circ$) and the other entrance beam angle (β) is varied. $I_1 = I_2 = 1.4 \text{ W/cm}^2$.


FIG. 5. Power spectrum of Fig. 4

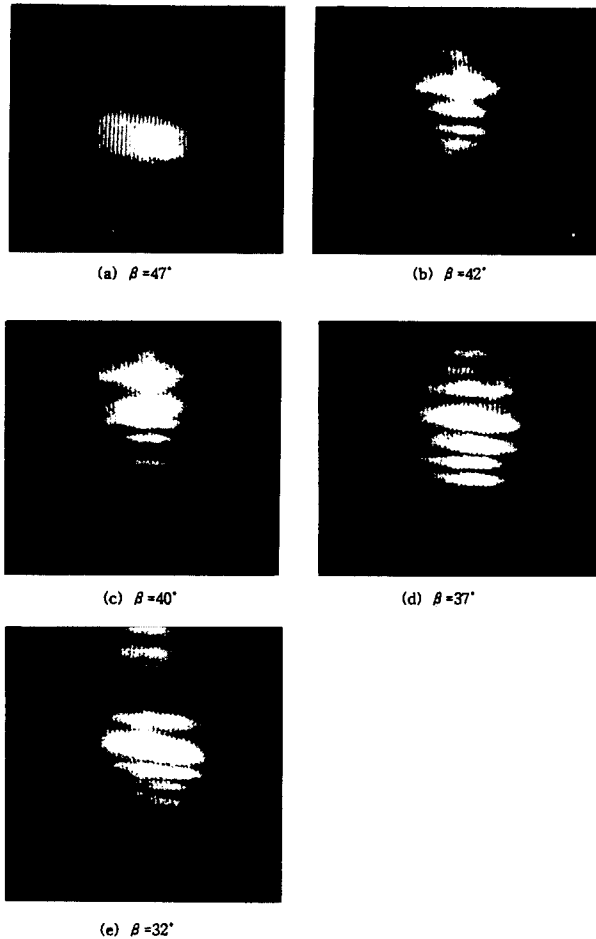


FIG. 6. Spatial pattern of PC when one entrance angle is fixed ($\alpha = 20^\circ$) and the other entrance beam angle (β) is varied.

creased. The spatial pattern moves and the temporal signal is the result of movement of the spatial pattern. The pattern in Fig. 6(b) moves one way uniformly, and the temporal signal is periodic. In Fig. 6(c), the motion of the pattern is more complex as the entrance angle is decreased. The movement of the spatial pattern is due to the DPCM domain drift [12]. In reference [12], the DPCM domain movement is verified by the electro-optic method. In our experiment, the excited nonlinear grating moves uniformly when the interaction region is small. But the motion of the nonlinear grating becomes irregular as the interaction region is increased.

Next, we tested the spatial correlation of the PC beam to check the stability of the spatial pattern when the transverse interaction region of two beams is changed. We fixed the entrance angle ($\alpha = 20^\circ$, $\beta = 37^\circ$) and the launching location of the two beams and changed the entrance beam diameter to change the transverse interaction region. The transverse interaction region is related to the Fresnel number [10]. The Fresnel number is defined with beam diameter as fol-

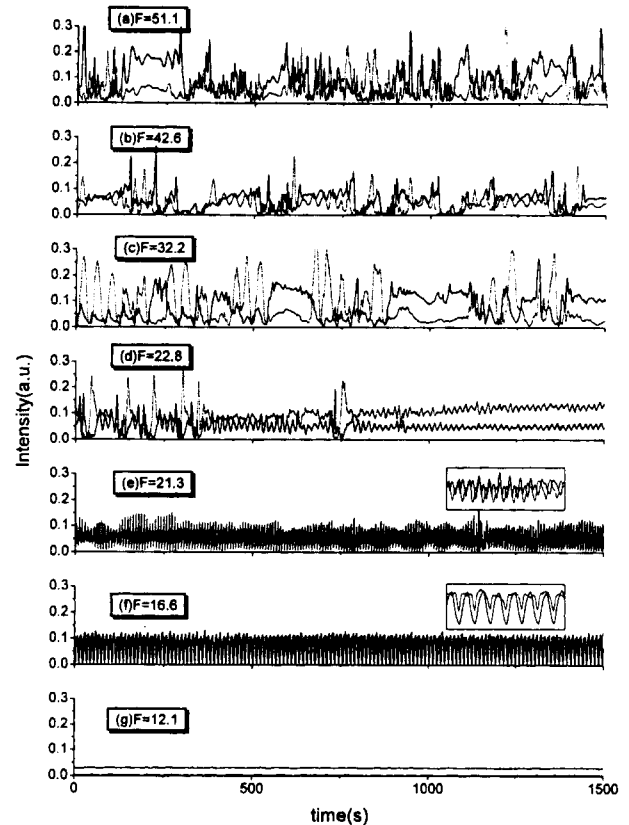


FIG. 7. Temporal Behavior of two different points in the PC beam as a function of Fresnel number. The entrance angles of two beams are fixed to $\alpha = 20^\circ$ and $\beta = 37^\circ$.

lows,

$$F = \omega_1 \omega_2 / \lambda d, \quad (5)$$

where ω_1 and ω_2 are the beam diameters of each entrance beam, λ is the wavelength and d is the thickness of the crystal. We checked the spatial correlation of two different points using temporal signals as a function of Fresnel number. The experimental result is shown in Fig. 9.

In Fig. 7 the dotted and solid line signal indicate the temporal signals of different points in the PC beam. From Fig. 7 the temporal behavior becomes more complex as the Fresnel number is increased (that is, the transverse interaction region increased). In the experiment the local intensity fluctuations were measured at the two points, separated by approximately one half the diameter of Aperture A_1 . Fig. 8 is the power spectrum of Fig. 7. In this figure, we can see the frequency of each point is almost the same when the Fresnel number is small. But as the Fresnel number is increased, the frequency of each point becomes different. That is, the temporal signal of each point behaves independently. This indicates the spatial correlation is decreased as the Fresnel number is increased. We calculate the spatial correlation index [13]. The correlation

function is defined as follows,

$$C(\mathbf{r}_1, \mathbf{r}_2, \Gamma) = \frac{\sum_{n=1}^N [I(\mathbf{r}_1, n) - \bar{I}(\mathbf{r}_1)][I(\mathbf{r}_2, n + \Gamma) - \bar{I}(\mathbf{r}_2)]}{S(\mathbf{r}_1)S(\mathbf{r}_2)}, \text{ and } S(\mathbf{r}_j) = \sqrt{\sum_{n=1}^N [I(\mathbf{r}_j, n) - \bar{I}(\mathbf{r}_j)]^2}, \quad (6)$$

where \mathbf{r}_1 and \mathbf{r}_2 are the two locations in the wave front at which the local intensity fluctuations are measured in PC beam, n is the running time and Γ is the time delay, N is the total time and I and \bar{I} are the intensity and the averaged intensity of PC beam.

The spatial correlation index is defined as follows,

$$K(|r_1 - r_2|) = \text{Max } C(r_1, r_2, \tau), \quad \forall \Gamma. \quad (7)$$

The experimental result of spatial correlation index is shown in Fig. 9. The larger K means the higher temporal and spatial correlation. From Fig. 9, the K becomes negligible as the Fresnel number is increased over F_c (~ 22.8). This shows that the spatial pattern of the PC beam becomes unstable as the transverse interaction region is increased over F_c . If the interaction region is more increased, the output beam of the crystal loses its pure PC property and becomes distorted.

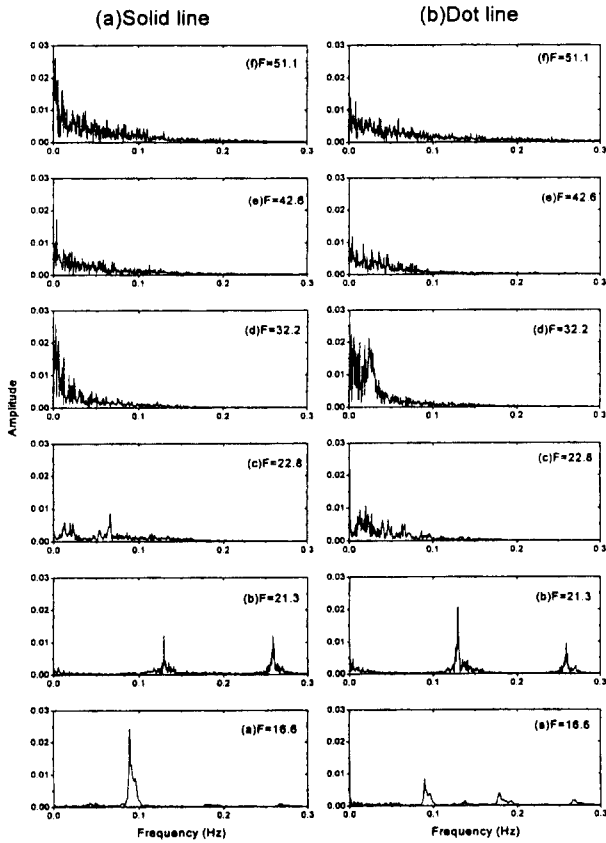


FIG. 8. Power spectrum of temporal signals at different points in the PC beam as a function of Fresnel number. The entrance angles of two beams are fixed to $\alpha = 20^\circ$ and $\beta = 37^\circ$.

These results are in accordance with Fig. 7 .

These phenomena are observed in conical emission. Fig. 10 shows the conical beam image. The left beam is the phase conjugate one and the right is the one passing through the crystal directly. We think that this phenomena is the intermediate process for transition to spatio-temporal chaos. But the spatiotemporal behavior in the conical emission beam is not understood

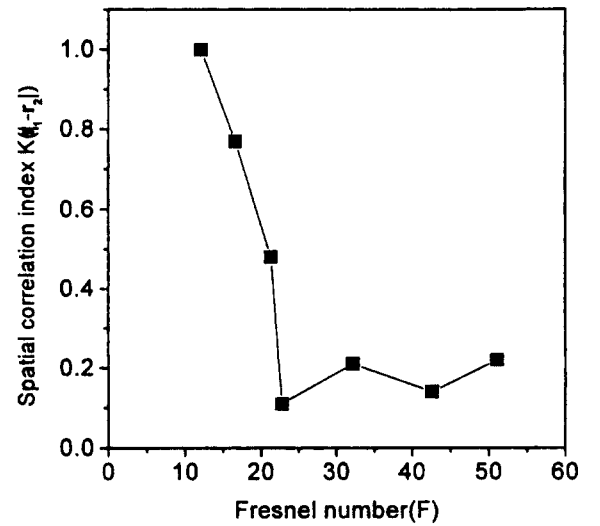


FIG. 9. Spatial correlation index as a function of Fresnel number.

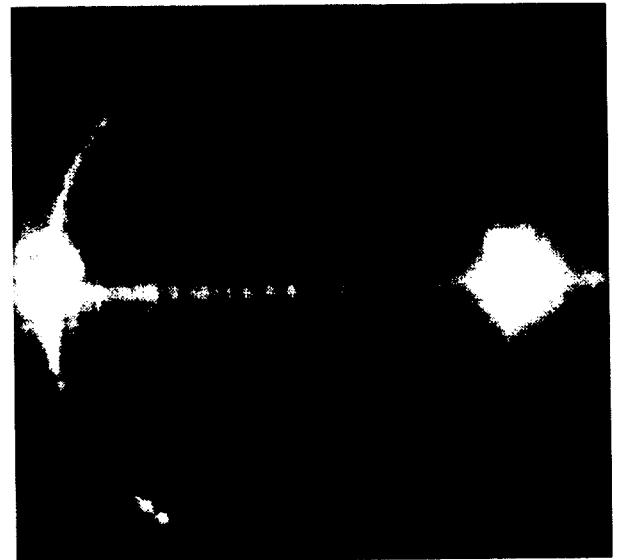


FIG. 10. The PC wave (left) and conical emission. The light on the right is the beam passing through the crystal directly.

well and such spatio-temporal instabilities are under currently investigation.

V. CONCLUSION

We have studied experimentally transverse and dynamical effects of DPCM with various interaction regions. The temporal behavior and spatial pattern of the PC beam becomes unstable as the interaction region is increased. The unstable behavior of the temporal signal is due to the increment of the unstable grating as the interaction region is increased. The chaotic temporal signal is due to the movement of the spatial pattern which is due to the drift of the DPCM domain. The drift becomes more complex as the interaction region is increased. Also we verified the spatial instability with spatial correlation index as the transverse interaction region is increased. Spatial pattern instability is also due to the increment of the unstable grating with increasing transverse interaction region. But this phenomena in conical emission is not understood well and such spatio-temporal instabilities are under current investigation.

ACKNOWLEDGMENTS

This research was supported by the Korea Research Foundation(1998-015-D00114).

REFERENCES

- [1] S. Sternklar, S. Weiss, M. Segev and B. Fisher, *Opt. Lett.* **11**, 528 (1984).
- [2] R. W. Eason and A. M. C. Smout, *Opt. Lett.* **12**, 51 (1987).
- [3] J. Feinberg, *Opt. Lett.* **7**, 486 (1982).
- [4] N. V. Bogodaev, V. V. Eliseev, L. I. Ivleva, A. S. Korshunov, S. S. Orlov, N. M. Polozkov and A. A. Zozulya, *J. Opt. Soc. Am. B* **9**, 1493 (1992).
- [5] A. A. Zozulya, M. Saffman and D. Z. Anderson, *Phys. Rev. Lett.* **73**, 818 (1994).
- [6] M. Segev, D. Engin, A. Yariv and G. C. Valley, *Opt. Lett.* **18**, 1828 (1993).
- [7] S. Orlov, M. Segev, A. Yariv and G. C. Valley, *Opt. Lett.* **19**, 578 (1994).
- [8] M. Cronin-Golomb, B. Fischer, *IEEE Electron.* **25**, 550 (1989).
- [9] D. J. Gauthier and D. Narum, *Phys. Rev. Lett.* **58**, 1640 (1987).
- [10] M. R. Belic, J. Leonardy, D. Timotijevic and F. Kaiser, *J. Opt. Soc. Am. B* **12**, 1602 (1995).
- [11] P. Yeh, *Introduction to Photorefractive Nonlinear Optics* (John Willy & Sons. Inc) Ch. 6, p. 237.
- [12] N. Wolffer and P. Gravey, *Opt. Commun.* **107**, 115 (1994).
- [13] S. R. Liu and G. Indebetouw, *J. Opt. Soc. Am. B* **9**, 1507 (1992).